Draft December 5, 2006

SNDICE: A Direct Illumination Calibration Experiment

A proposal to monitor and calibrate Megaprime at CFHT

K. Schahmaneche, E. Barrelet, C. Juramy + SNLS group

LPNHE, Universités Paris VI et VII

Summary

Precise photometric calibration of wide field imagers has become a major issue for many science objectives currently pursued with these instruments, such as the precise measurement of cosmological parameters from the luminosity distances to Type Ia supernovae, or the determination photometric redshifts.

The analysis of the data collected during the first year of the Supernova Legacy Survey (SNLS), has shown that the systematic uncertainties affecting the cosmological parameter measurements derived from Type Ia supernovae distances are currently dominated by photometric calibration uncertainties [2]. These uncertainties arise from (1) the determination of the instrumental zero points relative to the primary flux standard (Vega), the uncertainties affecting the measurements of the reference spectrum used to compare fluxes measured in different bands (Vega), and the uncertainties of the filter transmission curves. In addition, since Megacam is large mosaic imager, CCD to CDD relative calibration has to be precisely understood and monitored [4].

These uncertainties will get smaller as our understanding of the CFHT/Megaprime instrumental suite continues to improve, thanks to the vigorous observational calibration program that is currently being performed by the CFHTLS and SNLS collaborations. It is likely however that the photometric calibration uncertainties will remain the dominant part of the overall error budget at the end of the SNLS.

The classical approach (in fact, the only one until now) to calibrate science exposures is to rely on observations of field stars calibrated to a standard system such as Landolt [9] or Smith [10]). This approach has many advantages, including accounting for variations of the atmospheric and instrumental transmissions. However, in order to "break through the 1% precision barrier" it becomes necessary to explore a complementary approach, such as the one proposed by [3], based on performing an "instrumental" calibration of the overall observational setup (CFHT+Megaprime in our case), coupled with an "external" measurement of the atmospheric transmission.

With this proposal, we aim at performing the instrumental calibration and monitoring of Megaprime on CFHT, by building and operating a calibration system, based on the direct illumination of the primary mirror using commercial Light Emitting Devices (LED) [1]. We think such a project would give CFHT a lead role in exploring instrumental monitoring and calibration issues that are of extreme importance for future wide field projects. We estimate that the proposed system could be built and installed at CFHT within about a year after construction starts.

In chapter 1, we summarize the scientific justifications for building such a calibration system. The proposed instrumental setup is described in chapter 2 and its operation as well as the analysis of calibration data are described in chapter 3. Manpower, cost and schedule issues are discussed in chapter 4.

The main idea and most of details of the project we propose are adaptations for CFHT of principles of instrumental calibration for Sne experiments exposed in [1].

Contents

Chapter 1

Scientific Justification

The systematic uncertainties arising from photometric calibration of Megaprime at CFHT currently dominate the error budget in measuring cosmological parameters from luminosity distances to type Ia Supernovae. We review the systematic uncertainties that affect these measurements and discuss ongoing improvements and possible future improvements that would come from an instrumental calibration.

As discussed in [3], in addition to properly removing instrumental artifacts, fully characterizing the atmospheric transmission along the instrument line of sight is needed for "breaking through the 1% precision barrier". Obviously, this is an important part of the overall photometric calibration problem but we do not discuss it here. Rather we concentrate on improving the precision that can be achieved on the instrumental side, in measuring the camera uniformity, controlling its stability and *in fine* obtaining absolute colors and possibly an absolute photometric calibration.

1.1 The importance of photometric calibration in SNLS

The Supernova Legacy Survey is comprised of two components: an imaging survey to detect SNe and monitor their light-curves, and a spectroscopic program to confirm the nature of the candidates and measure their redshift.

The imaging is taken as part of the deep component of the CFHT Legacy Survey [6] using the 36 CCD/340 megapixels MegaCam imager [8].

The analysis of the data collected during the first year of the SNLS has shown that the systematic uncertainties affecting the cosmological parameters measured from Type Ia supernova distances, are currently dominated by uncertainties in the photometric calibration [2].

For a total systematic uncertainty on Ω_M of ± 0.032 (in a flat Universe), the 3 main contributions are respectively the determination of the individual zero points (± 0.024), the uncertainties on Vega spectrum (± 0.012) and the ones related to the filter transmission curves (± 0.007).

1.1.1 A Few Definitions

When we measure the flux of an object, the number of ADU in a given pixel could be expressed as follows :

$$N_{ADU_{x,y}}(t, \Delta t) = \int \phi(\lambda, t).T_{atm.}(Z, \lambda, t).A.T_{opt.}(\lambda, \alpha, t).T_{filt.X}(\lambda, \alpha, t, x, y).QE(\lambda, t, x, y).G.\Delta t.\mathrm{d}\lambda$$

where :

- x and y are the position of the pixel in the focal plane. We assimilate the position of the pixel to the center of the pixel and won't deal about the size of the pixels.
- t and Δt are the epoch of the exposure and the exposure time.
- $\phi(t)$ is the flux of the astronomical source at the entrance in the atmosphere. "Standard" stars won't have any time dependency.
- $T_{atm.}(Z, \lambda, t)$ is the transmission of the atmosphere which depends on the airmass Z, t and λ.
- A is the aperture of the telescope, the only constant !
- $T_{opt.}(\lambda, \alpha, t)$ is the transmission of all the optics (primary mirror, Wide Field Corrector and internal reflections). In first approximation, it depends on the rays incident angle with respect to the optical axis, α. This transmission could also evolve in time.
- $T_{filt.X}(\lambda, \alpha, t, x, y)$ is the transmission of the filter X used during the exposure. It should not depend on x and y if the filter thickness was perfectly uniform.
- $QE(\lambda, t, x, y)$ is the quantum efficiency of the pixel.
- $G.\Delta t$, the gain of the electronics. The dependence on Δt is a multiplicative factor assuming the linearity of the electronics that has to be checked.

As we want to measure ϕ, the calibration procedure aims at determining all the other terms individually or their product.

If we could observe an object of known reference spectrum, ϕ_{ref} (in erg/s/cm^2), we could perform the calibration by measuring this object at a time t' close enough to t to assume that the values of all the coefficients did not have time to vary.

We are going to use these definitions is the following sections.

1.1.2 Elixir image pre-processing, non uniformity of the camera and scattered light

All the images taken with Megacam are preprocessed at CFHT by the ELIXIR pipeline [7] developed, operated and maintained by the CFHT staff. The ELIXIR pipeline processes raw images and delivers "pre-processed" images that are:

- bias subtracted (pedestal removed),
- "flat-fielded" using twilight flat frames (pixel to pixel correction), and "defringed" (All flats and fringes patterns are produced for each run),

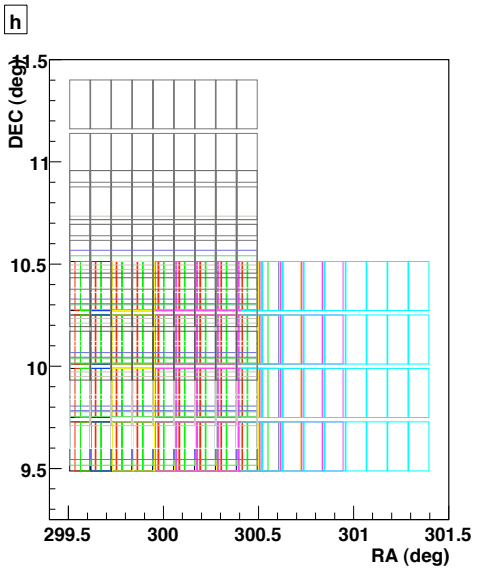

Figure 1.1: Dithering pattern of the observed dense stars field.

- Corrected from the non-uniformities of the imager photometric response (those non-uniformities arise from several effects (plate scale variations, scattered light and gain variations).

Elixir processed images are then distributed to users for science analyses. SNLS uses ELIXIR processed images.

Some uncertainties are inevitably introduced at this stage :

- The spectrum of the light used for the flat field must be close to the object we want to measure (or at least, close the night sky spectrum).
- There is some scattered light that will be taken into account in the flat field and not in the punctual source measurement.

To map the imager photometric response, dithered observations of dense stellar fields are performed on a regular basis. This allows one to intercalibrate the various parts of the camera by comparing many measurements of the same objects performed at different locations of the focal plane. The analysis of these data showed non-uniformities larger than what we could expect from "plate scale" variations. The excess is attributed to scattered light contributing significantly to the twilight flats.

But, it also showed remaining color term variations as function of the position on the focal plane. It could be interpreted as non uniformity of the filters thickness but this has to be proved.

1.1.3 Reference spectrum

After pre-processing procedure, the equation giving the number of ADU in a pixel become simpler. The x, y and α dependences can be removed :

$$N_{ADU_{x,y}}(t, \Delta t) = \int \phi(\lambda, t).T_{atm.}(Z, \lambda, t).A.T_{opt.}(\lambda, t).T_{filt.X}(\lambda).QE(\lambda, t).G.\Delta t.\mathrm{d}\lambda$$

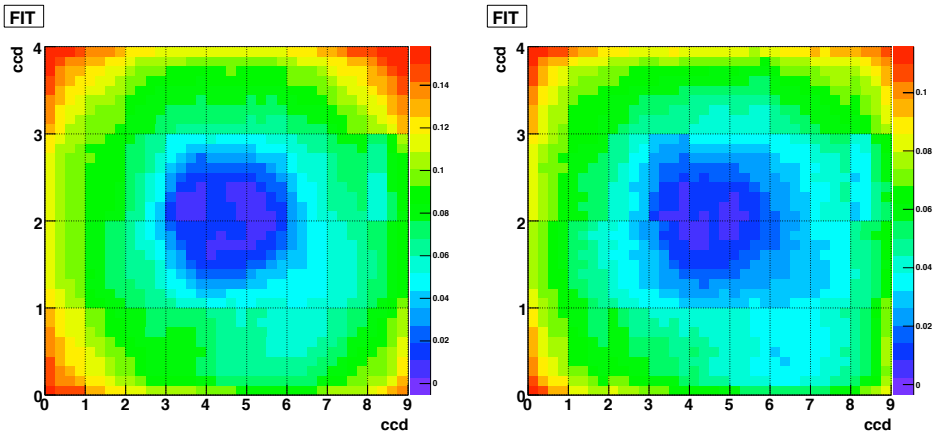

Figure 1.2: Non uniformity of the camera photometric response measured with dense star fields in two MegaCam filters r' and i'. The "correction" produced by Elixir is not applied on these images.

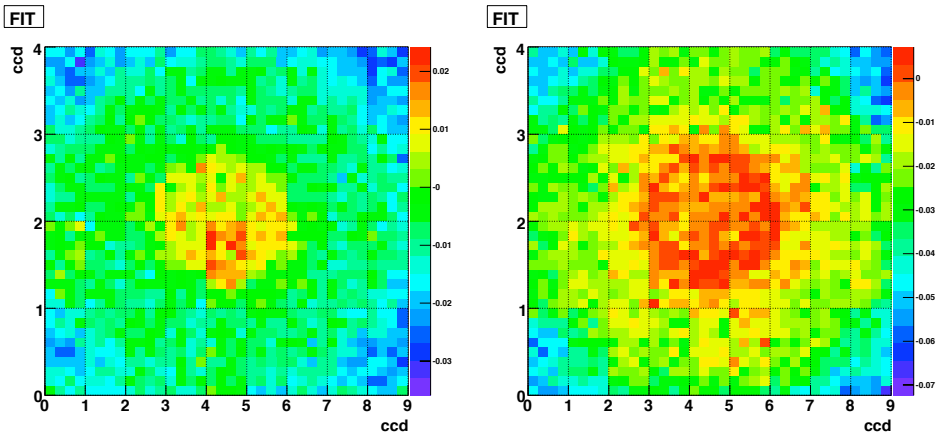

Figure 1.3: Filter mean wavelenght drift.

As it was said, a known spectrum of an astronomical source would allow one to determine in any filter X the product :

$$T_{atm.}(Z,\lambda,t).A.T_{opt.}(\lambda,\alpha,t).T_{filt.X}(\lambda).QE(\lambda,t).G$$

In theory, Vega could do this job. But first, there is some uncertainties in the measurement of its spectrum. And second, Vega is too bright to be observed directly by CFHT.

Figure 1.4 shows the ratio of two measurements of Vega (REF to come). The bold line is the spectrum measured by Bohlin with STIS/HST which was deduced by reference to white dwarfs whose spectra were modelized. The dash line is one of Hayes measurement which was obtained with ground based telescope and compared to black body radiations.

Differences are as big as 5% in the blue and greater than 10% above 900 nm are visible.

Furthermore, since measuring cosmology with SNe Ia relies on comparing SN fluxes at different redshifts, fluxes need to be compared in different filter band passes and therefore precise inter-calibration of these bands is essential. This is currently done also using Vega spectrum.

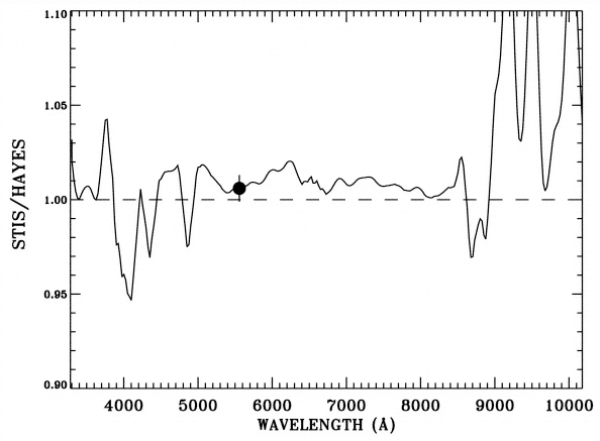

Figure 1.4: Ratio of Vega reference spectrum as measured by STIS (Bohlin) and Hayes (REF to come).

Figure 1.5 shows the spectrum of Vega as measured by Bohlin (REF to come) overlayed with the Jonhson-cousin filter set. The strongly varying flux and presence of strong absorption features particularly in the blue and near infrared make the use of Vega as reference for calibration far from optimal.

1.1.4 Tertiary reference stars catalog

Due to the impossibility of observing Vega with CFHT, we are obliged to refer to catalogues of sufficiently faint standard stars. The SNLS calibration scheme is the following [4].

To assign magnitudes to supernovae, we rely on magnitudes of reference stars located around the supernova: we measure the flux of these reference stars in the same images, with the photometry method used to measure the supernova flux, and we then derive the supernova magnitude. The reference objects have to be stars because we measure supernovae using PSF photometry, for sake of optimality.

To assign magnitudes to these reference stars which constitute a tertiary reference stars catalogue, we again rely on flux ratios and known magnitudes. Two sources of known magnitudes can be used to calibrate the SNLS: the Landolt catalog [9] (including the 95 Landolt standards which were re-measured by the SDSS collaboration [10]) and the SDSS science catalog that covers 2 among the 4 SNLS fields. As the nearby SNe Ia photometry were calibrated on the Landolt system, the SNLS calibration had to follow this path.

Using the coefficients we have defined, we can express this calibration step (the creation of the tertiary catalogue). Calling $\phi_{\mathrm{Lan}}(\lambda)$ the (unknown!) spectrum of one of the Landolt standard star, we have, after flatfielding, for the observation of this star with MegaCam :

$$N_{ADU_{x,y}\mathrm{Lan}}(t,\Delta t) = \int \phi_{\mathrm{Lan}}(\lambda).T_{atm.}(Z,\lambda,t).A.T_{opt.}(\lambda,t).T_{filt.X}(\lambda).QE(\lambda,t).G.\Delta t.\mathrm{d}\lambda$$

We want to calibrate one star of the tertiary catalogue of spectrum ϕ that doesn't neither depend on time ("standard star"). The same coefficients are involved:

$$N_{ADU_{x,y}}(t,\Delta t) = \int \phi(\lambda).T_{atm.}(Z,\lambda,t).A.T_{opt.}(\lambda,t).T_{filt.X}(\lambda).QE(\lambda,t).G.\Delta t.\mathrm{d}\lambda$$

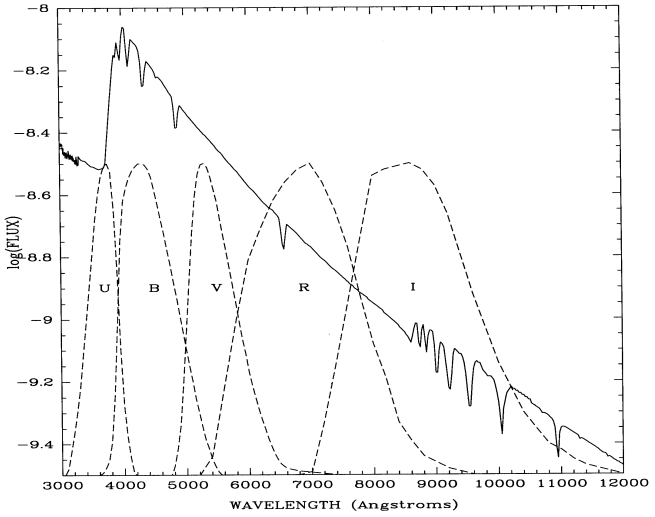

Figure 1.5: Vega spectrum with Johnson-cousin $UBVRI$ filter set

In addition, the known magnitudes of Landolt stars in one of the Landolt filter Y are expressed as a ratio of their flux to the flux of Vega, ϕ_{Veg} :

$$M_Y(\text{Lan}) = \frac{\int \phi_{\text{Lan}}(\lambda).T_{filt.Y}(\lambda).App(\lambda).\text{d}\lambda}{\int \phi_{\text{Veg}}(\lambda).T_{filt.Y}(\lambda).App(\lambda).\text{d}\lambda}$$

where $App(\lambda)$ is a global transmission function representing the apparatus used by Landolt during his measurement. To be more precise, it is exactly the Vega magnitudes in the Landolt system, i.e. with slight shifts.

The color equation between instrumental filter X and standard filter Y allows one to determine the zero points for each observation of each tertiary catalog stars in a given filter X. And this zero point,

$$Z_P(X,t) = 2.5\log_{10}\int \phi_{\text{Veg}}(\lambda).T_{atm.}(Z,\lambda,t).A.T_{opt.}(\lambda,t).T_{filt.X}(\lambda).QE(\lambda,t).G.\Delta t.\text{d}\lambda$$

is what CFHT should measure if Vega would have be in the field during the observation. The all procedure is explained in [4].

This zero point plays the role of a normalisation coefficient. Using mean transmission functions (whose product give an effective filter transmission function : $T_{filt.X\,\text{eff.}}(\lambda) = T_{atm.}(\lambda).A.T_{opt.}(\lambda,\alpha).T_{filt.X}(\lambda).QE(\lambda).G$), the zero point allows one to adjust the magnitude calculated to fit measured fluxes (in ADU).

To get a better accuracy, the Megacam-Landolt and Megacam-SDSS color transformations were checked by comparing synthetic and observed color-color diagrams. The synthetic color-color transformations were computed using the stellar spectra library [12] and models of the Megacam, SDSS and Landolt effective passbands. The observed color-color transformations were determined by comparing (1) SDSS and Megacam observations of the D2 and D3 fields and (2) Megacam observations of Landolt stars. The study showed that the effective models of the Megacam and SDSS filters in our possession reproduce the SDSS-Megacam color transformations well. It also showed that the effective passbands of the Landolt system are well reproduced by the specifications of [13] blueshifted by a few nanometers.

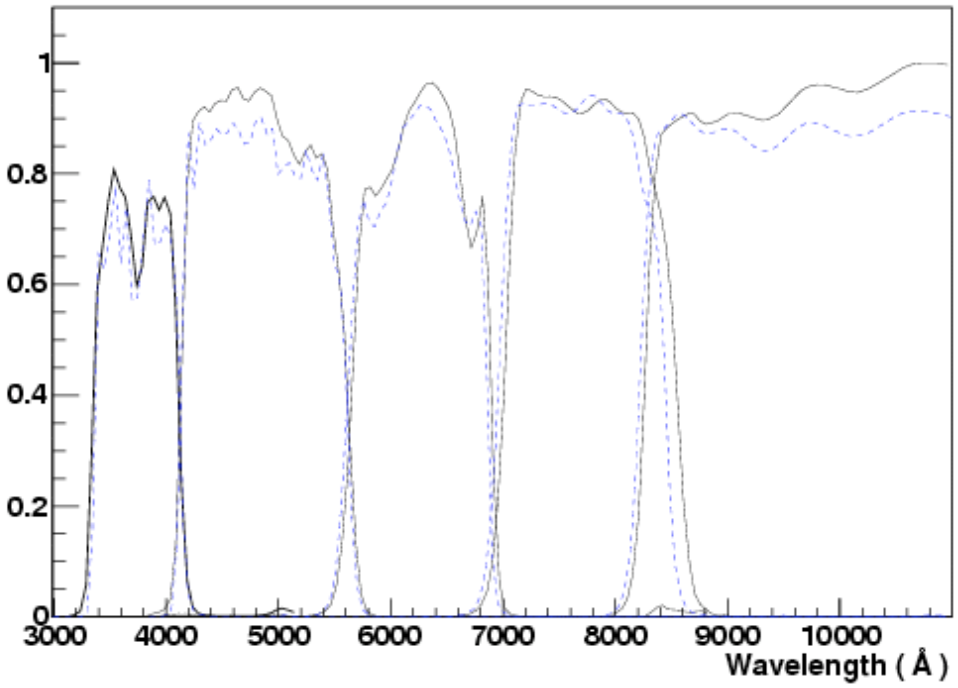

Figure 1.6: Comparison of the two determinations of the Megacam filters. The black plain line corresponds to the measurements made at CFHT. The blue dashed line was determined by the SAGEM/REOSC. The REOSC transmissions are slightly bluer than the CFHT ones, except for the u and g bands.

1.1.5 Filters band-passes

The Megacam filter band-passes were measured several times. Measurements were performed by the manufacturer (REOSC/SAGEM), and by CFHT. These measurements agree reasonably well in the u^* and g' bands but differ substantially in the r, i and z- bands as shown in Figure 1.6. The mean wavelength shift are 2.4 nm in r', 7.2 nm in i' and 5.2 nm in the z'-band.

Recently (summer 2006), the g', r' and i' filters were (re)measured at CFHT. These new measurements measure the filters in several positions and their averages are closer to the transmission provide by REOSC, which was explicitely an average over the filter area. The spatial variations of the bandpasses are sizeable (a few nm between center and corners) and a calibration and/or monitoring system should allow for the determination of such variations. Table 1.1 displays the average wavelength of the g, r and i filters as well as other relevant quantities.

1.1.6 Short term expected improvements

The CFHTLS and SNLS collaborations plans to observe simultaneously the four SNLS deep fields along with the HST fundamental spectrophotometric standards [11]. These well measured standard stars could then be used as flux references to perform the cross filter flux calibration of the instrument.

	g	r	i
$\bar{\lambda}$ REOSC[a]	4855	6240	7689
$\bar{\lambda}$ CFHT1[a]	4857	6273	7770
New measurements			
$\bar{\lambda}$ CFHT2[a]	4856	6252	7723
$\sigma(\bar{\lambda})$	6	8	26
index of refraction (± 0.2)	1.7	1.8	1.6
blue shift due to f/4 beam[b]	7	8	16
$\bar{\lambda}$ CFHT2[c]	4847	6244	7707

[a]Central wavelengths of the filter alone at normal incidence.
[b]We assumed an f/4 beam with the Megacam central obscuration
[c]Central wavelengths of the filter alone, in a f/4 beam

Table 1.1: Megacam filter band-passes.

1.2 Instrumental calibration

A complementary approach to using stars to calibrated the camera is to perform a precise instrumental calibration. This means to measure the transmission function of the different parts of the instrument in function of time: $T_{opt.}(\lambda, t)$, $T_{filt.X}(\lambda, t)$ and the product $QE(\lambda, t).G$.

Such an approach will provide us with a precise monitoring of the response function of the whole instrument as a function of wavelength as well as the precise measure of the filter edges

In addition, one could work to achieve the determination of the fluxes of the observed astronomical objects independently of any reference star using a calibrated source (absolute calibration). Closely related to this last point, a precise modeling of the atmospheric transmission, $T_{atm.}(Z, \lambda, t)$, is also mandatory.

From the photometric point of view, if it is difficult to estimate quantitatively how much we can gain, it is obvious that a better knowledge is necessary.

1.2.1 A stable multi-λ calibrated source

The main quality for a calibrated source that is required is to be stable and be able to cover the whole bandwidth of the instrument. Different complementary approaches are proposed. The first setup proposed by Chris Stubbs is based on a tunable laser illuminating a flat screen. In addition, we propose a calibrated multi-LED source that illuminate directly the primary mirror. What is common is the use of a calibrated detector (photo-diode) delivered by a specialized institute (NIST for example) to measure the incoming light flux.

1.2.2 Tunable laser

C. Stubbs developed an instrumental calibration setup that he tested on the CTIO-4m [3]. The tunable laser that he uses allows a fine sampling of the throughput of the instrument. The laser light is directed trough a blank screen on which the telescope focused. Using a photodiode calibrated by NIST, it's possible to maintain as a constant the number of photons entering the imager.

The measurement of the throughput of MegaPrime with this setup will be very informative.

But some aspects motivate for another complementary instrumental device. First, it is very important to be able to check regulary the stability of this throughput measurement which is hardly possible with something not with residence at the CFHT.

Second, with this setup, it is difficult to get uniform light beam. This is due to the screen that play the role of an extended secondary source.

Finally, the interest of measuring the scattered light would also request a more focused light beam.

That is why, we propose a calibration scheme based on a direct illumination of the primary mirror.

Chapter 2

Instrumental Setup

2.1 CFHT Optics

The imager, MegaCam, is mounted at the prime focus of CFHT. The parabolic main mirror of the telescope alone does not produce a good image of the whole field of view, and so a Wide-Field Corrector (WFC) is installed in front of the camera.

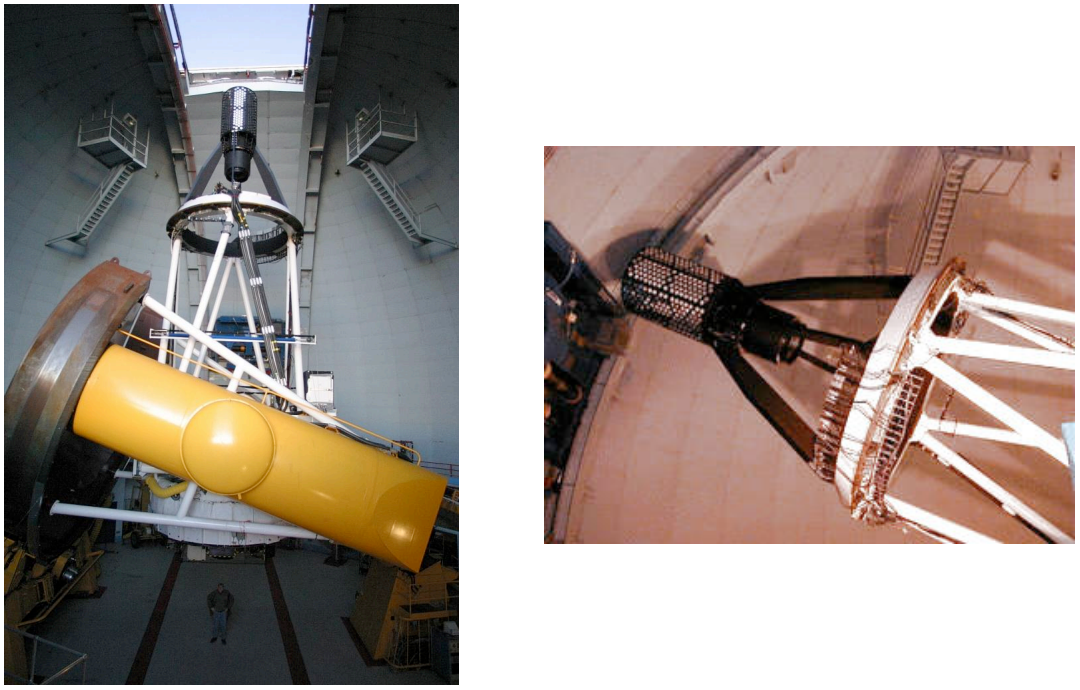

Figure 2.1: Views of the telescope and MegaPrime.

The 1 square degree imager is composed of 36 CCDs (2kx4k 13.5 μm pixels each) and has a 30 s readout time (using 2 channels per CCD). Megaprime currently has five broad-band filters, constructed by SAGEM/REOSC: u*, g', r', i', z'. Except for u* these filters were designed to match the SDSS filters as closely as possible.

Figure 2.2: Wide Field Corrector standing in front of MegaCam.

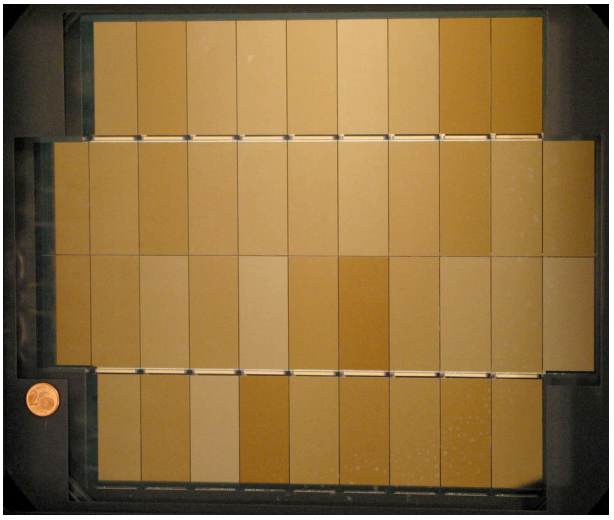

Figure 2.3: MegaCam CCDs mosaic.

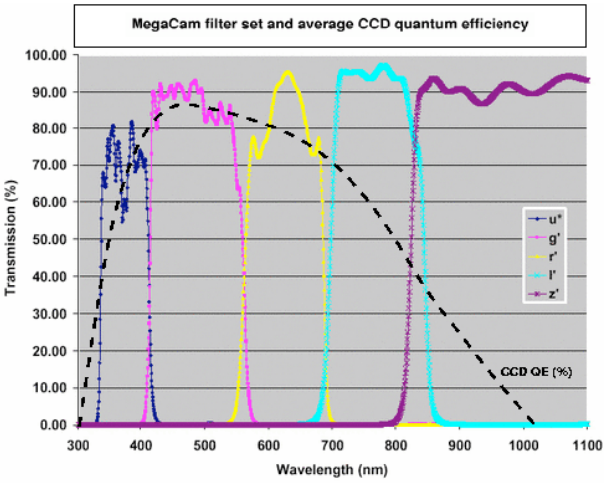

Figure 2.4: MegaCam filters and CCDs QE.

2.2 Principles of the project

The instrumental calibration device pecularities that we propose are the following:

- Direct illumination: the light sources are directly oriented towards the primary mirror. The light beam is well defined so that the scattered light is reduced and the uniformity on MegaCam is ensured.
- The light is coming from Light Emitting Diodes which are cold, stable and easy to control sources which is very important for monitoring.
- The light sources are absolutely calibrated and controlled redundantly by a cooled calibrated photo-diode intercepting the light entering MegaCam.

2.2.1 Beam Geometry

The LEDs will be gathered in a compact space close to Megaprime, at the level of the focal plane, so that illuminating directly the parabolic primary mirror, they will generate a uniform beam over the whole camera. The aperture of this beam will be of 2×3 degrees to illuminate Megaprime and the calibrated cooled photo-diode placed on one arm of the "spider".

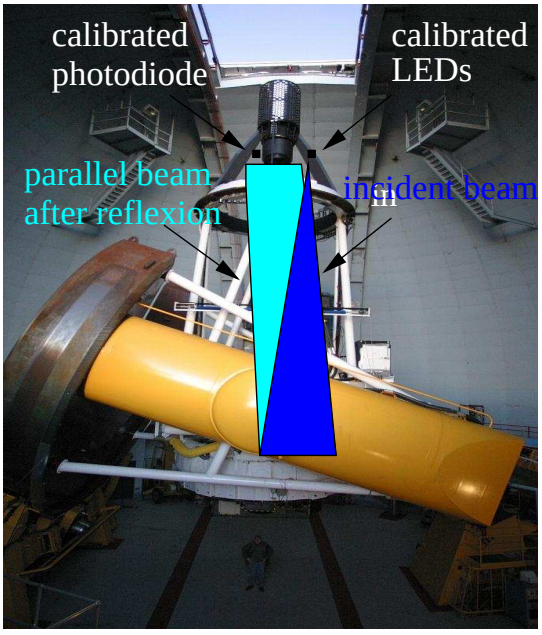

Figure 2.5: Calibrated sources and detectors.

It is important to note that an isotropic source with a given open angle α will always, after reflexion on the parabolic mirror, illuminate the same surface of radius $d = f \tan(\alpha)$ in the focal plane where f is the focal distance. This is partly why we can say that with this device, MegaCam will be uniformly illuminated.

The fact that the sources will be off-axis by a distance δx imply that the light will enter the wide field corrector with an incidence angle β such as $\tan(\beta) = \frac{\delta x}{f}$. For example, a distance $d = 0.75$ m gives $\beta \simeq 3$ degrees. An offset δz of the position of the source with respect to the focal length will introduce a dispersion ϵ in the incidence angle of the beam at the entrance of the wide field corrector. This dispersion will be of the order of $\alpha \times \frac{\delta z}{f}$. In the case of an aperture of the initial beam $\alpha = 3$ degrees, and an offset of $\delta z = 10$ cm, the dispersion will be: $\epsilon \simeq 0.02$ degrees.

This dispersion concern only incidence angles. The illumination will stay a constant.

2.2.2 Monitoring of the instrument

To monitor the instrument, we have to calibrate the LEDs which mean to know precisely their luminosity for a given current, at a given temperature of the dome. The explanation of the calibration of the LEDs source will be found in the next chapter.

To have a redundant measure, we will also install a calibrated photo-diode close to MegaCam. The calibrated detector will be at the same distance of the source as the CCDs.

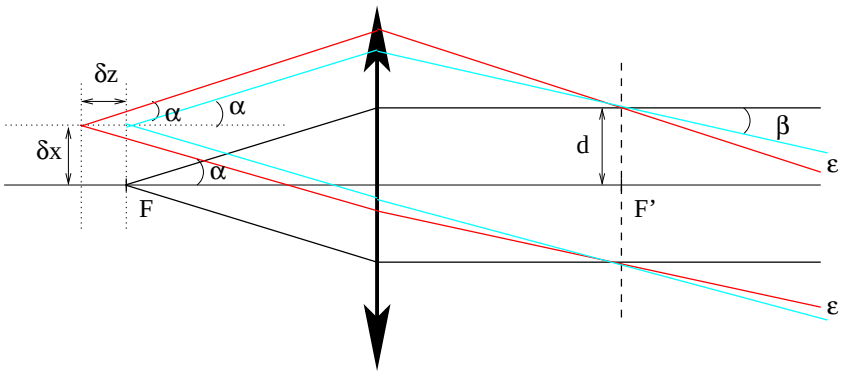

Figure 2.6: Geometry of the beam for an aperture α, an off axis distance δx and and offset δz.

That is why it must be cooled to lower the dark current and be able to measure very low light fluxes.

2.2.3 Sampling of MegaCam bandwidth

LED spectra are not monochromatic ($\frac{\Delta\lambda}{\lambda} \simeq 7\%$). This prevents from having a fine wavelength sampling of the instrument response, but on the other hand, this will avoid fringes on the MegaCam images.

The device we propose will be composed of 20 LEDs which spectra will go from UV to near infrared. The MegaCam 5 filters (u',g',r',i',z') cover the band-with from 300 nm to 1000 nm. This means that the throughput of the instrument could be measured and monitored for each of the 5 filters at 4 different wavelengths.

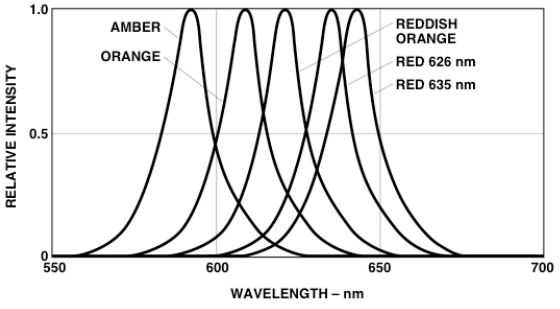

Figure 2.7: Example of LED spectra covering the r' filter.

We explain in the next section how we can get an isotropic source with LEDs, how stable are their spectrum and how we measure that stability.

2.2.4 "Relative" and "absolute" calibration - "absolute colors"

In addition to the monitoring of MegaCam, the major objective of the project is the "relative" calibration of object between the different filters. The known LEDs spectra will play the

role of a comon reference spectrum. This will lead to the "absolute colors" of the SNe (ie the color of the SNe without any reference to the color of another spectrum).

Let's express the total number of ADU per second of a SNe Ia of redshift z at peak magnitude in a filter X, measured at the epoch t with a PSF fitting procedure :

$$N_{ADU_{sn,X}}(t) = \int \phi(\lambda,t).T_{atm.}(Z,\lambda,t).A.T_{opt.}(\lambda,t).T_{filt.X}(\lambda,t).QE(\lambda,t).G.\mathrm{d}\lambda$$

And for another SNe Ia of redshift z' in a filter Y, measured at an epoch t' is :

$$N_{ADU_{sn',Y}}(t') = \int \phi'(\lambda,t').T_{atm.}(Z',\lambda,t').A.T_{opt.}(\lambda,t').T_{filt.Y}(\lambda,t').QE(\lambda,t').G.\mathrm{d}\lambda$$

Assuming the knowledge of the instrument transmission and its evolution in time, and an equivalent knowledge of the atmospheric transmission, we will be able to compare these two fluxes although these fluxes were obtained in different filters. This will allow to compare peak magnitudes of SNe Ia at different redshifts, observed in different bands without astronomical reference spectrum.

Of course such a program could be achieved with a competitive accuracy only with a good modeling of the atmospheric extinction.

In a first step, let's say that the comparison of this instrumental fluxes clibration with reference stars calibration will essentially display the atmospheric effects ($T_{atm.}(Z',\lambda,t')$) and the systematic effects due to simplifying hypotheses.

To conclude this part, one can note that the need of such a cross calibration between filters (the "absolute colors") is not only needed by the cosmologists using SNe Ia. All comparisons of objects of the same class at different red shifts involve the same requirement at some level. For example, the galaxies photometric redshifts are based also on cross filters calibration. The typical uncertainty of a galaxy photometric redshift does not require a precise cross-filter calibration, but large sample averages (as weak shear studies requires) are sensitive to systematic biases.

2.3 Instrumental Device

LEDs and photo-diodes have been used together in particle physics experiments for calibration purpose. A precision and stability of 0.2% has been achieved together for the light emitted by the LED and the light detected by the photo-diodes [**?**]. Thus, similar devices will be of great use for calibration purpose of astronomical instruments.

The device we propose is rather simple in its conception [1].

2.3.1 LEDs module

The principle of the DICE experiment developed therein [1] is the direct illumination of the telescope. One have to find a stable, isotropic and with a narrow spectra light source. Light Emitting Diodes with non diffusive plastic cap are such light sources. These LEDs must have sufficient luminous power so that 10 000 ADU could be reached in each MegaCam pixel in a fraction of minute exposure.

Because the active part of a LED is very small (around 200 μm $\times$ 200 μm, cf Fig. 2.9), the directivity of the outgoing light beam is determined by the refraction in the matter

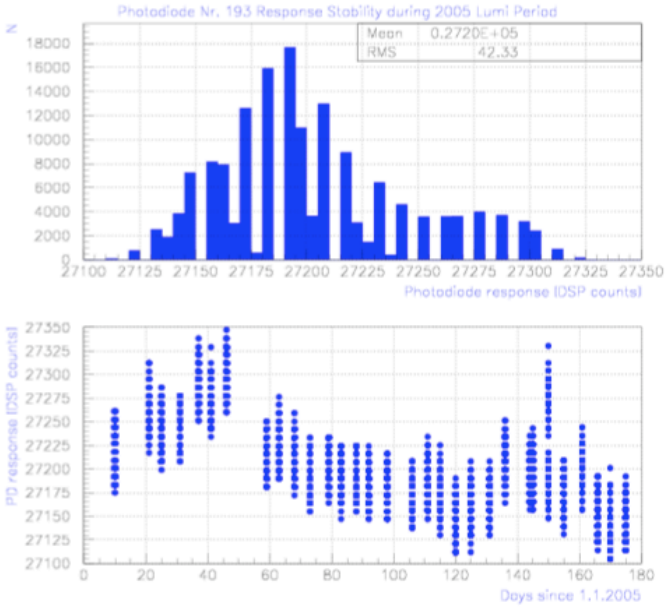

Figure 2.8: Calibration LEDs stability in the HEP H1 experiment over the 180 first year of 2005. A raw dispersion around the percent is shown.

surrounding the emitter. That is why, the "flat top" LEDs are commonly considered as lambertian emitters (Fig. 2.11).

The spectral distribution of a LED is easy to parametrize and smooth. Theoretically the shift of the central wavelength due to modification of the temperature is expected to be a few percent for several decades of degrees: for example, a shift of 5 nm for a 660 nm LED, and a 8 nm increase in the peak wavelength for a 950 nm LED as temperature increased from 0 to 50 degrees (REF to come).

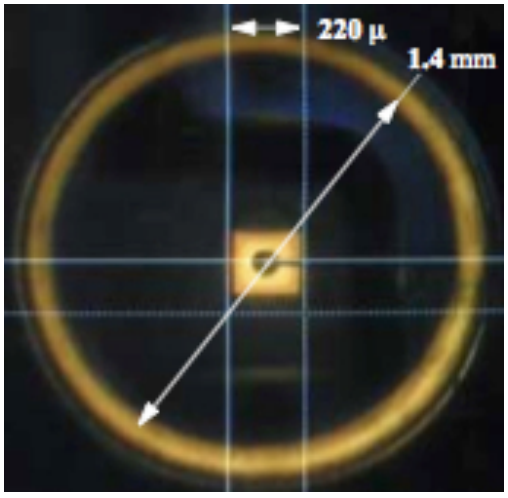

Figure 2.9: The active central part of a "flat top" LED.

The compact LEDs module will consist of approximatively 20 LEDs (not totally fixed) coverings the visible spectral range, from 300 nm to 1000 nm, and as many control off-axis

photodiodes (see fig 2.11). There will also be a temperature controller (thermistor or diode). The electronic card that will controls the LEDs and measure the currents of the photo diodes will be put far away from this head module to avoid heat dissipation in the telescope beam. This can be achieved because all the current going and coming from this LEDs head are transportable (several tens or hundreds of mA).

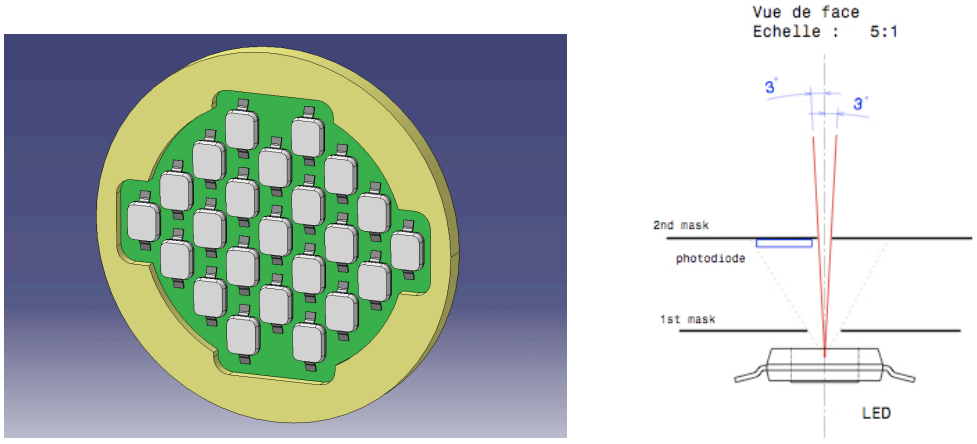

Figure 2.10: Possible design for the future LEDs head. The disk diameter is 70 mm. And a diagram of a 3 degrees beam configuration with the off-axis photodiode monitoring the emitted light at the source level.

The off-axis photodiodes could be Hamamatsu S1337 photo-diodes (good efficiency over the all visible spectral range). They will be disposed close to the LEDs (one for each LED) like on Fig. 2.10.

2.3.2 Beam Generation

The uniformity of the beam is a consequence of the "flat top" design of the LED that create an isotropic field. It is however necessary to mask the sides of the LED to keep only the light coming from the central emitting region and reject internal reflecting light. This gives a point source. Then, a second mask define the beam angle.

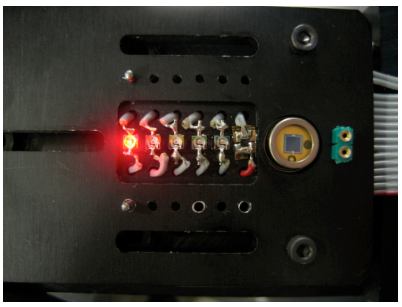

Figure 2.11: Prototype of 6 LEDs "flat top" which spectra covers roughly the r' filter and .

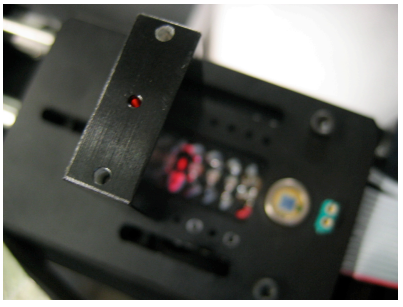

Figure 2.12: Prototype with the mask defining a beam of 2 degrees.

We are currently measuring the flux generated by our protoype and we are checking that the beam is isotropic below 1% level.

2.3.3 Cooled large area photodiode

The necessity to cool a large area photodiode in order to suppress dark current is justified by the small photocurrent generated. To achieve this, a thermo-electric cooler and a temperature sensor are used (see Hamamatsu S3477 series). We have several options for the amplification of the low photocurrent. A Low Current Amplifier(LCA) adapted to the photo-diode is the most convenient solution.

It can be implemented with a commercial LCA with ultra low input bias current(few fA), in order to monitor photocurrent waveforms of transient LED illumination. The practical problem is that we have found only one such LCA (LCA-30-1T 10fA) and it has a fixed gain which does not cover the whole photodiode signal range.

Alternatively, an off-the- shelf picoammeter(Keithley Model 617 and 65143 fA) gives more versatility and performance. In our test bench we have developed a solution cumulating the advantages of both apparatus. It uses a dual gain amplifier connecting the analog output of Keithley 617 Programmable Electrometer to two 16 bits digitizers. This provides a system adding a 0.5 Mhz/21 bits waveform digitizer to a Keithley pre amplifier (low-input-bias-current/low-noise/programmable-gain/calibrated). On this line we are developing an ASIC integrating an ultra-low input bias current pre amplifier with the dual gain amplifier and digitizer in order to equip several diodes on the same focal plane. We expect 1/1000 electrical accuracy and a precision $< 1/1000$ with light-distance varying over a factor of 10 (current over a factor of 100). This corresponds to what is achieved with our current voltage measuring chain. Their radiance versus distance relation offers a calibration of the pA range, in principle more accurate than Keithley's electrical calibration (2% accuracy).

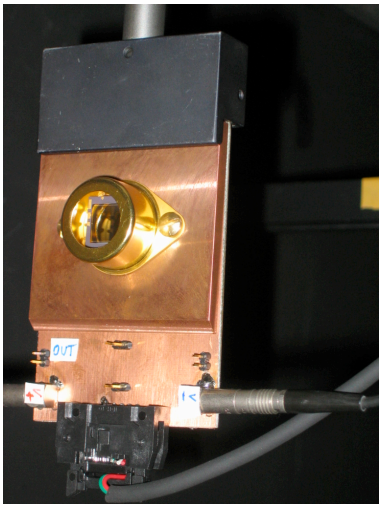

Figure 2.13: Cooled (Peltier effect) photodiode (Hamamatsu).

2.3.4 Electronics

The readout card will be placed far away enough so that its generated heat will not perturb the telescope beam. It will be connected to the "LEDs head" by a multiple wires cable (42 = 20 times 2 for LEDs and associated photo diodes + 1 for the thermal control + the mass). On the opposite side, it will be connected to a PC by an Ethernet link.

This card will be driven by an FPGA (Xilinx) controlling the 20 DAC (12 bits) generating the current of the LEDs and reading via a multiplexer the photodiodes currents encoding using a 16 bits ADC.

This FPGA will also do the acquisition of the temperature of the "LEDs head" and the acquisition of the cooled calibrated photo diode that will be placed at the level of MegaCam, in the beam of the LEDs.

2.3.5 Data acquisition

An Ethernet link will connect the FPGA, which will concentrate all the informations and command. This is totally sufficient as we estimate the maximum data rate below 1 Mb/s.

The acquisition software will be developed in labview environment. All the variables (LEDs currents, temperature of the LEDs head, current of control photodiodes, current of the calibrated large area control photodiode) will be monitored.

Control Command: SNDICE/MegaCam DAQ interface

The connection with MegaCam DAQ could be limited. For example, a common clock signal and a shutter signal could be enough. At a raw level, the command of SNDICE (which LED is light on and when) and MegaCam (exposures) could even be dissociated.

The SNDICE DAQ will produce a file containing mean and rms values for all the control variables monitored during any MegaCam exposures.

Header keywords

These data calibration files could be merged with MegaCam images via the introduction of instrumental calibration "keywords" in the header of the calibration images. All the calibration analysis would then only rely on image files.

2.4 Test schedule

It is of course crucial to test the main features that have been described on a test bench in Paris (Fig. 2.14).

Considering the LEDs source, the main tests that have to be achieved are the following :

- measure the flatness of the LEDs light beam on the focal plane (ie : isotropy of the beam),
- obtain a stable lignt with LED current control and of-axis photocurrent control,
- measure the spectral distribution variation of the LEDs light in function of time and temperature,

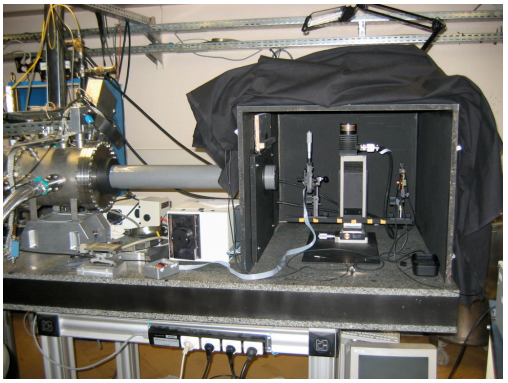

Figure 2.14: First test bench in Paris. One can see an X,Y motion device in front of a tube connected to a cryostat in which is a "focal plane" with CCD and Photodiodes.

- same measure for the intensity of the beam, ie : determine relation between voltage, current, temperature and emitted light power.

Complementary tests have also to be done for the CLAP :

- measurement and amplification of few fA/cm^2 signals,
- calibration transfer from NIST photodiode using CLED.

On our primary test bench , we are currently measuring tthe isotropy of the beam. One can see very preliminary results on figures 2.15 and 2.16.

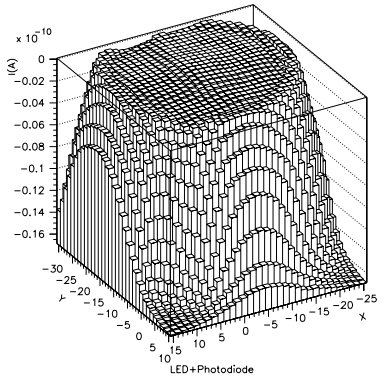

Figure 2.15: First raw measurement of a LED beam created by two consecutive masks.

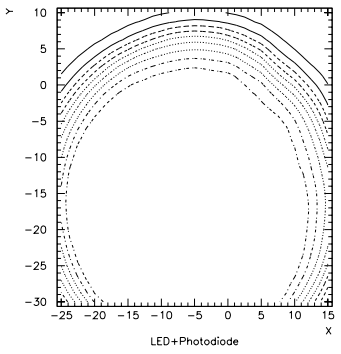

Figure 2.16: 10% level contour of the same beam.

2.5 Sources and detectors calibration

To be able to have an absolute calibration of the instrument, LEDs and the cooled photo-diode will be absolutely calibrated with the help of a calibrated photo-diode certified by the NIST.

2.5.1 NIST photo-diode

The calibrated photodiodes delivered by NIST are not able to measure very low luminosity. But we can use such a NIST calibrated photodiode to calibrate our LEDs source and then transfer this calibration to the cooled large area photodiode. We aim to do this with a calibration bench.

2.5.2 Calibration bench

The calibration bench that will allow us to perform the absolute calibration of our source and detector will be a two stage bench. A first one, 2m50 long will permit to specify and calibrate the LEDs using the NIST photo-diode (the integral radiometric calibration([1]) of the LEDs source) and then transfer the calibration from the LEDs to the cooled photo-diode. The transfer of calibration will be done by increasing the distance between the LEDs and the photo-diodes, and check the distance to flux relation.

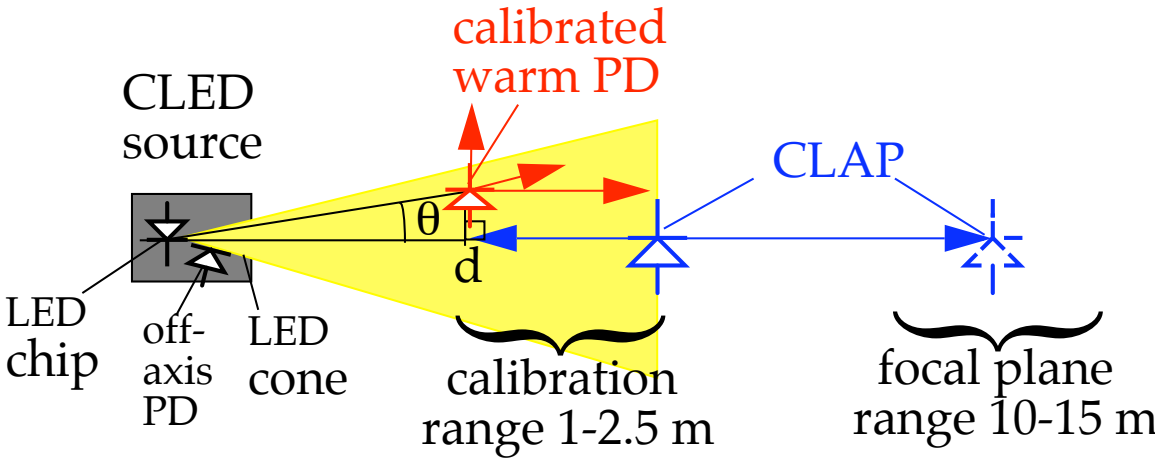

Figure 2.17: Diagram of the calibration bench for the CLED (Calibrated Light Emitting Diode) source and the CLAP (Cooled Large Area Photo-diode).

Chapter 3

Operation and Data Analysis

3.1 Measurements description

The calibration signal will be controlled at different points : from its generation to its detection. The figure ?? describe the differents part of the beam and where are the measurements.

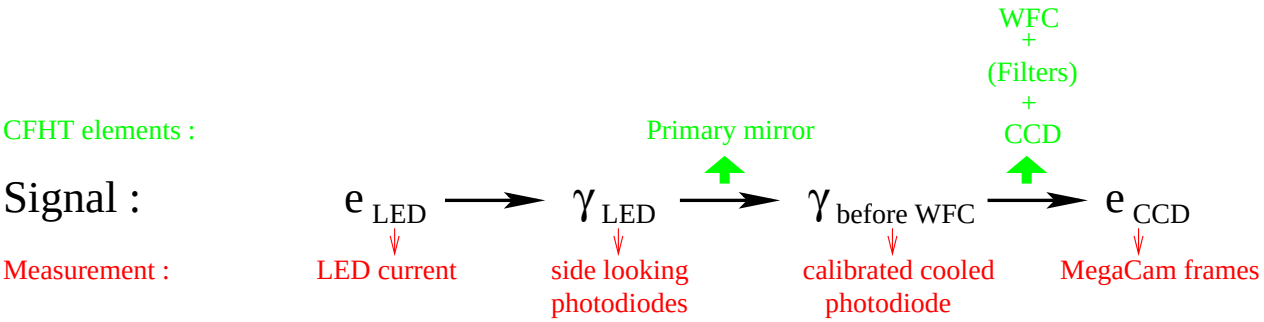

Figure 3.1: Diagram of the calibration control points.

The acquisition procedure could be the following :

1. Switch the selected LED(s) light on. It will be possible to light on one LED alone or several at the same time. The intensity is also selected by fixing the LED current.
2. As several values are monitored (LED current, light from the LED(s) at the level of the source, light at the level of the WFC), the second step is to check that all these values are what expected (ie with respect to reference stored values).
3. Then one can take several frames with MegaCam with different or same exposures.
4. It is then necessary to take MegaCam frames with LED light off to estimate the background noise.
5. Then, monitored values are added to MegaCam images headers (mean and rms of: temperature of the LEDs source, intensities of the lit LEDs, current of the corresponding off-axis photodiodes and current of the calibrated cooled large area photodiode).

After this procedure, all the following analysis will be done starting from MegaCam images containing calibration informations.

One can measure, $R_{x,y}(\lambda_k)$, the throughput of the instrument for a given pixel (of coordinate x, y) at the 20 calibration mean wavelength λ_k. This value can be expressed as follow :

$$R_{x,y}(\lambda_k, t) = \frac{\int \phi_{\mathrm{LED}_k}(\lambda).T_{opt.}(\lambda, \alpha, t).T_{filt.X}(\lambda, \alpha, t, x, y).QE(\lambda, t, x, y).G.\mathrm{d}\lambda}{\int \phi_{\mathrm{LED}_k}(\lambda)\mathrm{d}\lambda}$$

This value is in fact the ratio of the number of ADU in a given pixel to the number of photons hitting the primary mirror that will then enter the pixel (of area $S = 13.5 \times 13.5 \mu\mathrm{m}^2$) during the exposure time (Δt).

This second number is known, because of the LEDs absolute calibration, for a given LED current (I_{LED_k}) and corrected for the measured temperature (T). For an exposure time Δt, we have :

$$N_\gamma(I_{\mathrm{LED}_k}, T, S, \Delta t) = \int \phi_{\mathrm{LED}_k}(I_{\mathrm{LED}_k}, T)\frac{S\Delta t}{{d_f}^2}\mathrm{d}\lambda$$

where $\phi_{\mathrm{LED}_k}(I_{\mathrm{LED}_k}, T)$ is the known flux of the isotropic source per solid angle and f_d the focal distance of the primary mirror. The ratio $\frac{S}{{d_f}^2}$ is the "plate scale constant" for a pixel. The previous relation is then available even if the LED source is not exactly at the focal plane level.

So:

$$R_{x,y}(\lambda_k) = \frac{N_{ADU_{x,y}}(I_{\mathrm{LED}_k}, T, \Delta t)}{N_\gamma(I_{\mathrm{LED}_k}, T, \Delta t)}$$

A redundant check is of course obtained using the cooled calibrated photo-diode. In that case, one has to take into account the reflectivity on the mirror and the ration of the area of the pixel to the one of the photodiode.

3.1.1 Non uniformity of the camera and scattered light

For each frame, the ratio $R_{i,j}(\lambda_k)/R_{i_{ref},j_{ref}}(\lambda_k)$ will lead to a normalized flat field. This will reveal all the non uniformity of the camera as with SNDICE device the light beam is uniform.

Furthermore, the well defined beam getting out of the LEDs source reduce the scattered light to a minimum. Comparing (ie dividing) the flat field obtained with SNDICE with the current twilight flat or science master flat, will give an estimation of the amount of scattered light that enters the images in different case (science, dome, twilight).

3.1.2 "Varying Coloured" Flat Fields

Having several LED spectra contented in one filter band-with, will allow to modify the spectra of the light source used to make flat fields and so to be able to reproduce the main color of the science frames. This is crucial for the i' and z' bands where fringes frames are usually deduced from the comparison between flat frames obtained with long time exposure (science images) and short time exposure (dome or twilight flat fields) but with quite different light (night sky in a case and sun light or lamp in the other).

3.1.3 Filters

As there is a position in the Megacam filter wheel that doesn't have any filter, with measurement with and without a given filter, one will be able to measure the transmission of each filter for each pixel and be able to look at the non uniformity of the filters.

3.2 Calibration Program

We present here a way of using our calibration device. As the luminosity of the LEDs allow to reach the 10000 adu in Megacam with 10 s and taking into account the readout time of 30 s, we can estimate that the all procedure described just above (all the LEDs one after the other with off light exposures $= 20 \times 2 = 40$ exposure) will take $1600\,\mathrm{s} \simeq 30\,\mathrm{mn}$.

For the flat fields with a night sky color like, it should last $5 \times 2 = 10$ exposures, ie around 5 mn.

If the darkness of the CFHT dome is not good enough to do such calibration measurement during daytime, these procedures could be done as follow :

- each night: a sky color like flat field in each band,
- each month: a general calibration,
- once a year: a measurement of the filters transmission.

Furthermore, during nights where the dome must be kept closed, all the calibration procedures could be done. And when large extinction avoid any science, one could profit to study this extinction with the CFHT as a calibrated telescope.

3.3 "Absolute Colors" Determination

Using flat obtained by SNDICE, the flat field correction applied to each image will simultaneously level the images in the different filters to the same number of photons.

Then, assuming a good modeling of the atmospheric transmission, the known spectrum of the LEDs source could replace Vega spectrum (or other astronomical standard) as reference for inter calibration between filters. This determination of the "absolute colors" of the SNE (ie without reference to any reference star colors) could be a crucial step in SNe cosmology as in all other topics based on the comparison of the same object at different red shifts, like the determination of photometric red shifts of galaxies.

Of course, all of this is strongly dependent of progress on the modeling of atmosphere transmission but, at least, such a procedure will help in investigating the systematics.

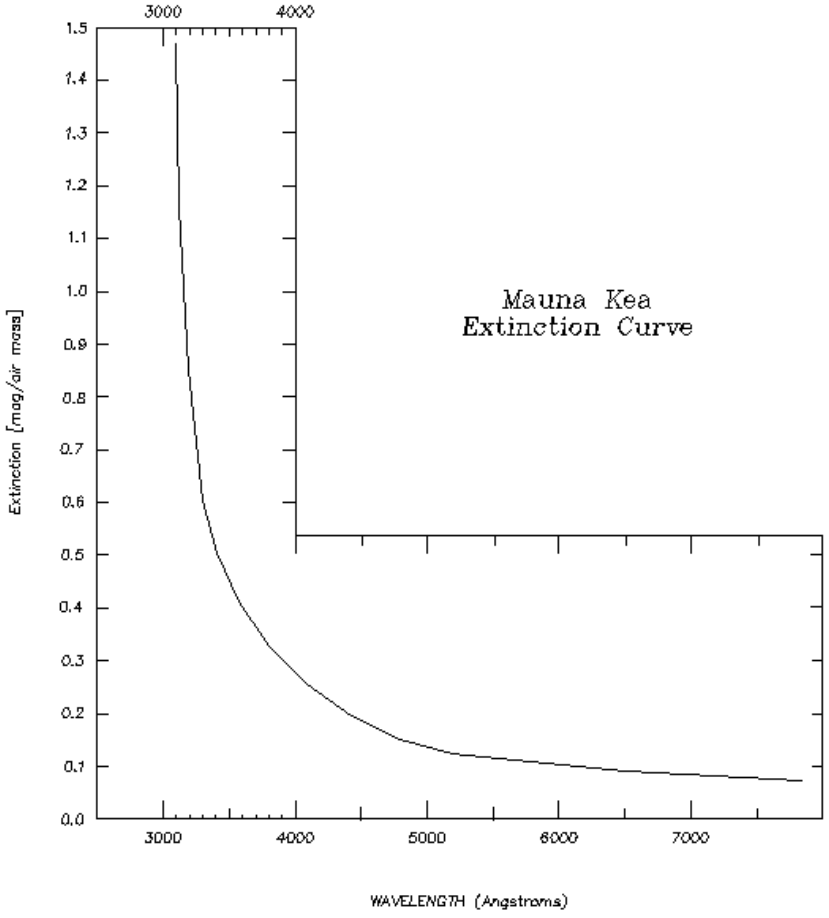

Figure 3.2: Mean extinction coefficient versus wavelength for Mauna Kea (from the CFHT webpage).

Chapter 4

Project Organization and Schedule

4.1 Manpower

The team in charge of the project is composed of phycisists (K. Schahmaneche, E. Barrelet, C. Juramy), SN Team (N. Regnault, J. Guy, P. Astier, D. Hardin, R. Pain, P. Antilogus), electronics and mechanics engineers (Resp. tech: D. Vincent - Mechanics: W. Bertoli, C. Evrard - Electronics/ASIC conception: R. Sefri, H. Lebbolo - Electronic card: A. Vallereau - FPGA programming: P. Bailly - DAQ: J-F Huppert).

4.2 Budget

	2006	2007	2008	2009	Total
DEVICE					
Electronics	5k euros	5k euros			10k euros
FPGA	5k euros	5k euros			10k euros
ASIC	10k euros	5k euros			15k euros
DAQ	5k euros	5k euros			10k euros
Cooled photodiode	5k euros				5k euros
NIST photodiode		5k euros			5k euros
Calibration bench		10k euros			10k euros
Contingency		5k euros			5k euros
Maintenance			5k euros	5keuros	10k euros
MISSIONS					
Missions to Hawaï		15k euros	10k euro	10k euro	35k euros
Shipping and installation		10k euros			10k euros
TOTAL	30k euros	65k euros	15k euros	15k euros	125k euros

Table 4.1: Budget from 2006 to 2008.

4.3 Schedule

Figure 4.1: Schedule (first part).

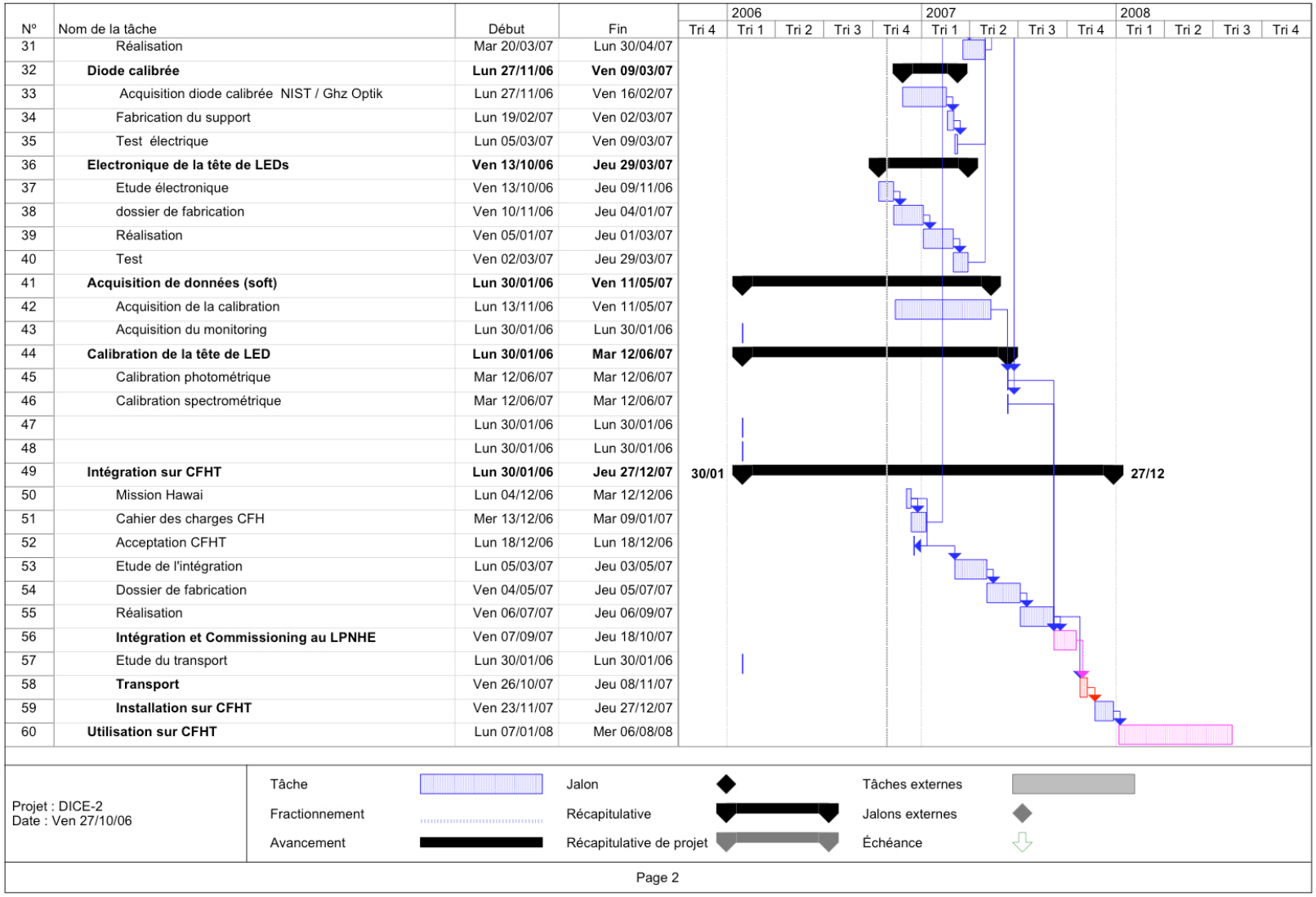

N°	Nom de la tâche	Début	Fin
31	Réalisation	Mar 20/03/07	Lun 30/04/07
32	**Diode calibrée**	**Lun 27/11/06**	**Ven 09/03/07**
33	Acquisition diode calibrée NIST / Ghz Optik	Lun 27/11/06	Ven 16/02/07
34	Fabrication du support	Lun 19/02/07	Ven 02/03/07
35	Test électrique	Lun 05/03/07	Ven 09/03/07
36	**Electronique de la tête de LEDs**	**Ven 13/10/06**	**Jeu 29/03/07**
37	Etude électronique	Ven 13/10/06	Jeu 09/11/06
38	dossier de fabrication	Ven 10/11/06	Jeu 04/01/07
39	Réalisation	Ven 05/01/07	Jeu 01/03/07
40	Test	Ven 02/03/07	Jeu 29/03/07
41	**Acquisition de données (soft)**	**Lun 30/01/06**	**Ven 11/05/07**
42	Acquisition de la calibration	Lun 13/11/06	Ven 11/05/07
43	Acquisition du monitoring	Lun 30/01/06	Lun 30/01/06
44	**Calibration de la tête de LED**	**Lun 30/01/06**	**Mar 12/06/07**
45	Calibration photométrique	Mar 12/06/07	Mar 12/06/07
46	Calibration spectrométrique	Mar 12/06/07	Mar 12/06/07
47		Lun 30/01/06	Lun 30/01/06
48		Lun 30/01/06	Lun 30/01/06
49	**Intégration sur CFHT**	**Lun 30/01/06**	**Jeu 27/12/07**
50	Mission Hawai	Lun 04/12/06	Mar 12/12/06
51	Cahier des charges CFH	Mer 13/12/06	Mar 09/01/07
52	Acceptation CFHT	Lun 18/12/06	Lun 18/12/06
53	Etude de l'intégration	Lun 05/03/07	Jeu 03/05/07
54	Dossier de fabrication	Ven 04/05/07	Jeu 05/07/07
55	Réalisation	Ven 06/07/07	Jeu 06/09/07
56	**Intégration et Commissioning au LPNHE**	Ven 07/09/07	Jeu 18/10/07
57	Etude du transport	Lun 30/01/06	Lun 30/01/06
58	**Transport**	Ven 26/10/07	Jeu 08/11/07
59	**Installation sur CFHT**	Ven 23/11/07	Jeu 27/12/07
60	**Utilisation sur CFHT**	Lun 07/01/08	Mer 06/08/08

Figure 4.2: Schedule (second part).

Bibliography

[1] [E. Barrelet and C. Juramy 2006]Direct Illumination Led Calibration for Type Ia Supernovæ Photometry, LPNHE 2006-02

[2] [Astier et al. 2006]The Supernova Legacy Survey: Measurement of Ω_M, Ω_Λ and w from the first year data set, P. Astier et al., A&A (2006) 447, 31-48

[3] [Stubbs and Tony 2006]Toward 1% Photometry: End-to-end Calibration of Astronomical Telescopes and Detectors, C. W. Stubbs and J. L. Tonry, astro-ph/0604285

[4] [Regnault et al. 2006]Photometric Calibration of the Supernova Legacy Survey fields, N. Regnault et al., astro-ph/0610397

[5] [Stubbs et al. 2006]Prelimnary Results from Detector-Based Throughput Calibration of the CTIO Mosaic Imager and Blanco Telescope Using a Tunable Laser, C. W. Stubbs et al., 2006, astro-ph/0609260

[6] [CFHTLS 2003]main cfhtls reference

[7] [Magnier and Cuillandre 2004]E. A. Magnier and J-C. Cuillandre, 2004, PASP 116, 449

[8] [Boulade 2003]O. Boulade et al., 2003, SPIE 4841, 72

[9] [Landolt 1992]A. U. Landolt, 1992, AJ 104, 340

[10] [Smith 2002]J. A. Smith et al, 2002, AJ 123, 2121

[11] http://www.stsci.edu/hst/observatory/cdbs/calspec.html

[12] [Pickles, 1998]A, J. Pickles, PASP, 110, 863

[13] [Bessel, 1990]M. S. Bessel, PASP, 102, 1181